A study on arching mechanism in trapdoor model test and equivalent discrete element simulations

Umair Ali Naqvi and M. Otsubo

Institute of Industrial Science, The University of Tokyo, 4-6-1 Komaba, Meguro-Ku, Tokyo 153-8505, Japan

ABSTRACT

The complex interaction of underground structures with the surrounding soil has long been studied due to their importance in practical geotechnical engineering. Prior researchers have reported that the stress distribution on a buried structure varies sensitively with the settlement of surrounding subsoil. However, certain soil parameters influencing the soil-structure interaction need to be clarified. In this contribution, trapdoor model tests using a soil box with multiple movable base plates mounted with load cells were conducted. Spherical glass beads were used as analogue to soil particles to assess fundamentals of arching resistance mechanism. To understand particle scale responses during the trapdoor test, the discrete element method (DEM) simulations were also performed. In the numerical DEM analyses spherical particles with the equivalent diameter range and the material properties were considered for better comparison. It was found that the earth pressure distribution varies with varying height to width (*H/B*) ratio, and arch formation is observed with increasing the *H/B* value. Arching action is further confirmed by evaluating the shear stress distribution on the base plates and the surface settlement of the model ground. These observations are in good agreement between experiments and DEM analyses.

Keywords: trapdoor test; discrete element method; arching; earth pressure; glass beads

1 INTRODUCTION

Massive underground infrastructure in big cities across the world necessitates the study of complex soil-structure interaction. Buried structures such as box culvert, sewerage pipelines and other utility lines may face an increased earth pressure due to relative settlement of backfill material, leading to distortion or damage to the buried structure (Fig. 1).

The ratio of increased earth pressure to the initial pressure on a buried structure, can increase up to 1.6 according to Japan road association (1999), determined empirically based on field measurements. However, the influence of mechanical properties of backfill material is not considered in the design code. This requires further understanding of the mechanism of earth pressure development.

Kuwano and Ebizuka (2010) found that the distribution of earth pressure on a buried structure is sensitive to the density of surrounding subsoil, the burial depth of the structure and the amount of relative settlement of subsoil. The failure mechanism for deep and shallow trapdoors was discussed by previous researchers including Costa et al. (2009).

Chevalier et al. (2009) and Rui et al. (2016) showed that the peak shear strength of material influences the arching pattern using DEM analyses.

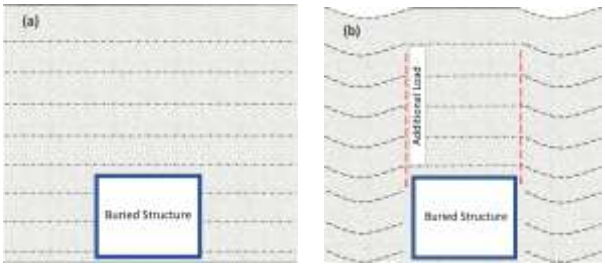

Fig. 1. Buried structure, e.g. box culvert (a) after construction (b) increase in pressure on structure due to differential settlement.

2 TRAPDOOR MODEL TESTS

2.1 Test apparatus

A soil box, representing trapdoor test, was prepared using five movable base plates (Fig. 2). Details of experimental setup for the same apparatus is given in Kuwano and Ebizuka (2010). Dimensions of the trapdoor apparatus are 700 mm (L), 293 mm (W), and 555 mm (H). Width of each movable plate (B) is 100 mm consisting of 5 sub-parts and each sub part contains a load cell that measures both the normal and shear forces. In total, 25 load cells were installed. Sand papers were pasted on the top surface of the base plates to magnify the shear stress measurement. The settlement of base trapdoor plates was measured using an external displacement sensor, and the surface settlement was measured using three laser displacement sensors.

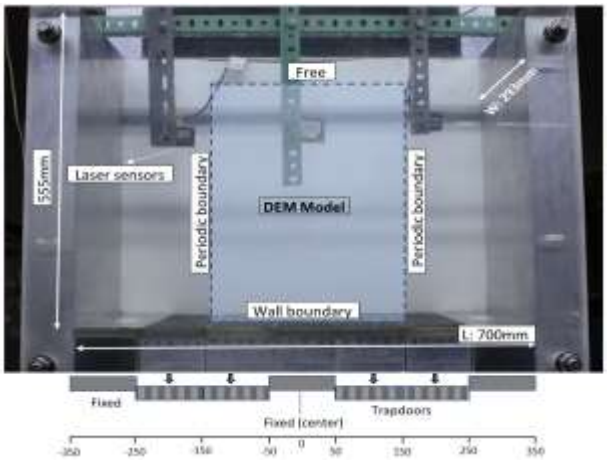

Fig. 2. Trapdoor test apparatus and equivalent DEM model.

Table 1. Test cases.

Test case	H (mm)	*H/B*	e	α_{peak}	α_{10mm}
Model-1	100	1.0	0.605	1.44	1.24
Model-2	200	2.0	0.608	1.83	1.61
Model-3	300	3.0	0.604	2.04	1.97
Model-4	400	4.0	0.592	2.24	2.13
DEM 1	44.2	0.44	0.624	1.21	
DEM 2	87.3	0.87	0.617	1.38	
DEM 3	175	1.75	0.611	1.72	
DEM 4	261	2.61	0.610	2.02	
DEM 5	348	3.48	0.609	2.17	
DEM 6	434	4.34	0.608	2.24	
DEM 7	521	5.21	0.607	2.28	

2.2 Test conditions and material properties

Spherical glass beads with diameters ranging from 1.2 to 2.2 mm were used in the model tests as analogue to soil particles and the same diameters were used in DEM simulations. The specific gravity, the Poisson's ratio and the particle Young's modulus of the material are 2.5, 0.23, and 71.6 GPa, respectively.

Air (dry) pluviation method was used to prepare the model ground keeping a constant drop height of 100 mm, and the resultant void ratio (e) varied from 0.592 to 0.608 (Table 1). The sample heights (H) were 100, 200, 300 and 400 mm, giving *H/B* = 1.0, 2.0, 3.0 and 4.0, respectively, where B = 100 mm. Slightly larger density was observed for higher *H/B* values due to increased overburden pressure level. To visualize the ground deformation, colored glass beads layers were prepared. For each test, the elevation of the central base plate was fixed whilst lowering the other four plates with a constant rate of 1.2×10^{-6} m/s (Fig. 2).

3 DISCRETE ELEMENT SIMULATIONS

A modified LAMMPS (Plimpton 1995), 3-D DEM code, was used with the Oakforest-PACS system in the Joint Center for Advanced High-Performance Computing. The material properties of tested glass beads were used along with the Hertz-Mindlin contact model. A rigid base wall having the same material properties with the spherical particles was used with lateral periodic boundaries, representing the middle part of the model ground (Fig. 2). Spherical particles with an initial e of 3 were randomly generated and settled under gravity with an inter-particle friction coefficient (μ) of 0.05. Dimensions of the model ground were 300 mm (L) × 40 mm (W), whilst H varied. Resultant e ranged from 0.607 to 0.624 (Table 1).

Due to the presence of periodic boundaries in the lateral directions, DEM model consisted of three base plates with the central one as fixed. The μ value was increased to 0.35, and no damping was applied during lowering the base plates. To ensure quasi-static simulations, the rate of lowering was set to 1×10^{-4} m/s.

4 RESULTS

4.1 Earth pressure distribution

Peak earth pressure distribution measured on the base plates ($P_{z,peak}$) / initial pressure (P_zo) is presented in Fig. 3(a) where P_zo was calculated from the density and height of the model ground. The pressure ratio ($P_{z,peak}$ / P_zo) on the central plate increases with *H/B*, whilst the ratio on the side plates (i.e. lowering plates) decreases. The maximum and minimum pressures are observed at the inside and outside edges of the central plate, respectively.

This trend agrees with the DEM results (Fig. 3(b)) for *H/B* values ranging from 0.44 to 5.2. The pressure ratios are close to 1 at positions of ±150 mm for lower *H/B* values, indicating no change in pressure level due to the settlement. Referring to Fig. 3, the pressure distribution converges as *H/B* increases.

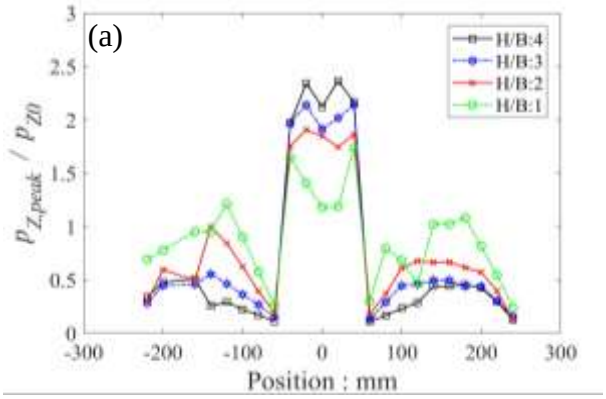

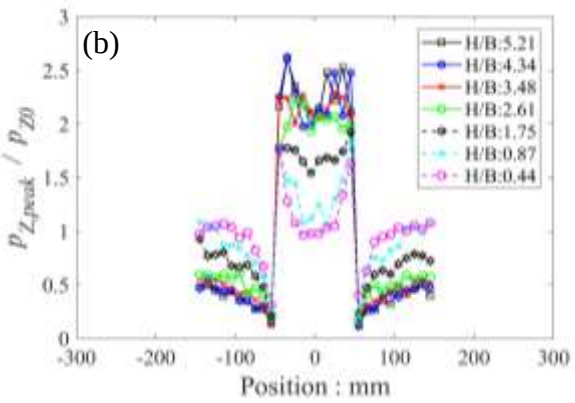

Fig. 3. Vertical pressure ratios (a) model test (b) DEM.

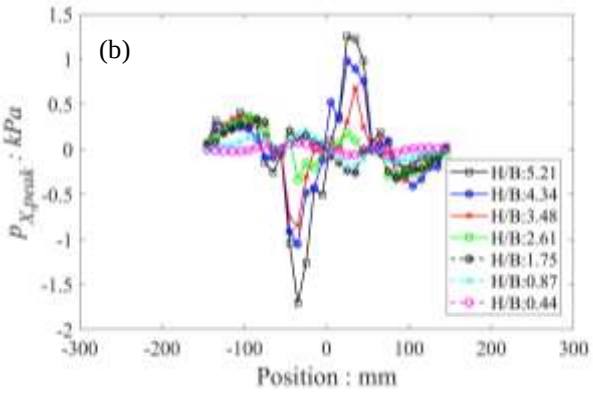

Fig. 4. Shear stress distribution for (a) model test (b) DEM.

4.2 Shear stress distribution and settlement

Shear stress distribution acting on the base plates was analyzed (Fig. 4). The positive value of shear stress in Fig. 4 corresponds to the force direction towards the positive side of position in Fig. 2.

The shear stress value is negative in the left half of the central plate at H/B = 3.0 and 4.0, whilst the same is positive in the right half. For the smaller H/B values, this trend is opposite or unclear. This is mostly due to a variation in the direction of particle movement with increasing H/B. This is further discussed below. The same trend is observed in the DEM results (Fig. 4(b)).

The settlement of the ground surface was analyzed using laser sensors and images. For smaller H/B values non-uniform settlement was observed (Fig. 5); however, uniform settlement of the top surface was confirmed in the model ground with higher H/B values. This can be linked to formation of an arch. For lower H/B, the differential settlement indicates that arching is not fully developed due to insufficient ground height. For higher H/B, arch action is maintained for greater movement of base plates; this causes uniform settlement at the top surface.

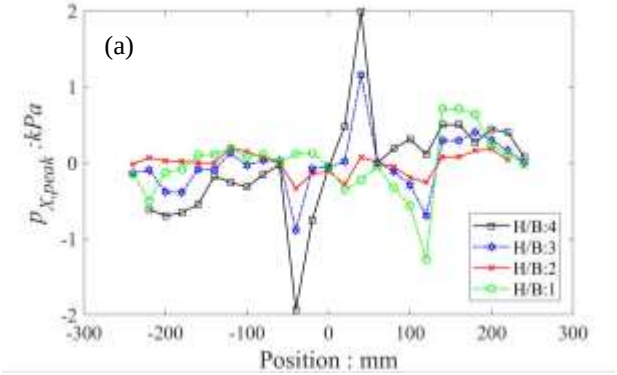

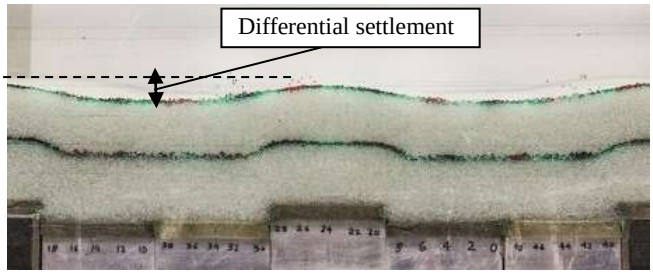

Fig. 5. Differential settlement for H/B = 1 (model test).

4.3 Particle movement associated with arching

Figure 6 illustrates schematically the direction of particle movement for higher and lower H/B values. Referring to Fig. 6(a) when two arches are developed above the side trapdoors, the particles above the arches are pushed towards the arches. This gives the shear stress on the central plate away from the center line (CL). In contrast, when an arch is not developed (Fig. 6(b)), the opposite movement of particles compered to Fig. 6(a) occurs and the trapdoor settlement causes differential settlement of the surface (Fig. 5). For both scenarios, the particles located along the CL stay at their initial location, which is confirmed as zero shear stress at position = 0 mm in Fig. 4.

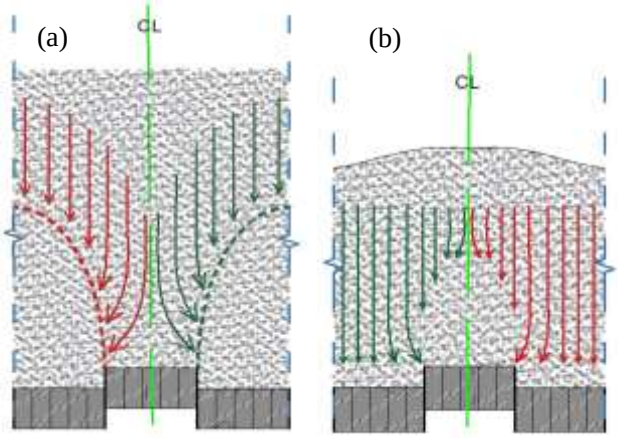

Fig. 6. Direction of particle displacement (a) with arching (b) without arching (positions from -150 mm to 150 mm).

4.4 Variation in α parameter

The ratio of the mean vertical pressure at the central plate (P_zc) to P_zo is defined as α (= P_zc / P_zo); this is a

measure of the increase in earth pressure acting to the buried structure. The α value increases with increasing the trapdoor settlement δ and *H/B* (Fig. 7). Referring to Fig. 7(a) the case for *H/B* = 4.0 exhibits a different trend at lower δ from the other experimental cases. This was caused by an initial slight difference in the elevation of the base plates; however, the peak and residual state responses were regarded as representative. The maximum values of α are similar with higher *H/B* values. This is probably related with development of an arch. Given that an arch is fully formed, no further increase in α is expected with further increase in δ.

Experimental results exhibit a softening response of α after the peak with increasing δ particularly for lower *H/B* values. This can be explained by the reduction in surcharge, as the model ground exhibits considerable differential settlement (Fig. 5 for *H/B* = 1.0). This can be a measure to assess the creation of an arch. Kuwano and Ebizuka (2010) showed a clear peak strength for dense Toyoura sand, which is not evident in this study, probably due to use of spherical particles.

Referring to Fig. 7(b) for the DEM results, the trapdoor settlement δ is limited up to 0.25 mm; thus, the post peak softening is not observed.

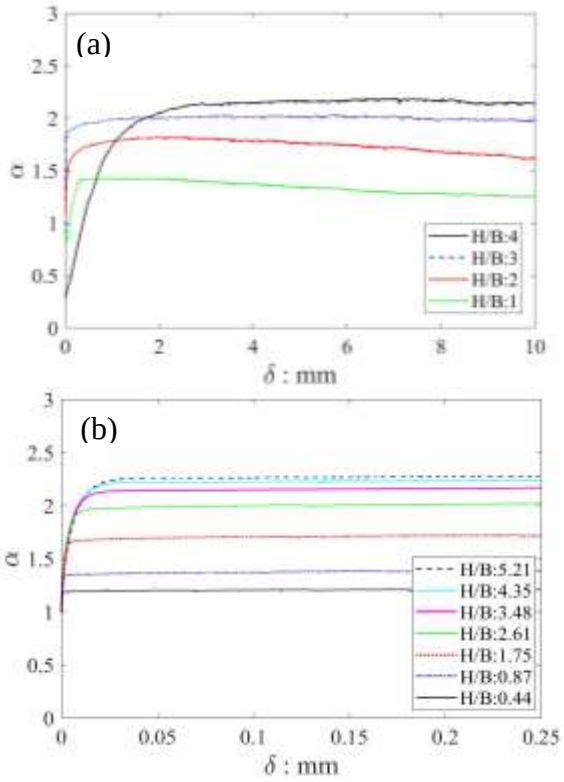

Fig. 7. Variation in α with settlement (a) model tests (b) DEM.

Figure 8 summarizes the maximum value of α (α_{peak}) for both experiments and simulations. The α_{peak} values obtained using Toyoura sand (Kuwano and Ebizuka 2010) and the design code (Japan Road Association 1999) are also compared in Fig. 8. The overall trend is similar amongst experimental cases and DEM analyses where α_{peak} increases almost linearly with increasing *H/B* up to 2. For further increase in *H/B*, α_{peak} increases non-linearly, and the rate of increment decreases. The design code underestimates α for the range of *H/B* examined. The α_{peak} values for dense Toyoura sand are larger compared with spherical glass beads at a similar void ratio; this is probably caused by particle shape. However, both cases approach α_{peak} = 2.5 to 3 as *H/B* increases. Note that the maximum possible α_{peak} is 3 for the configuration of trapdoor examined in this study.

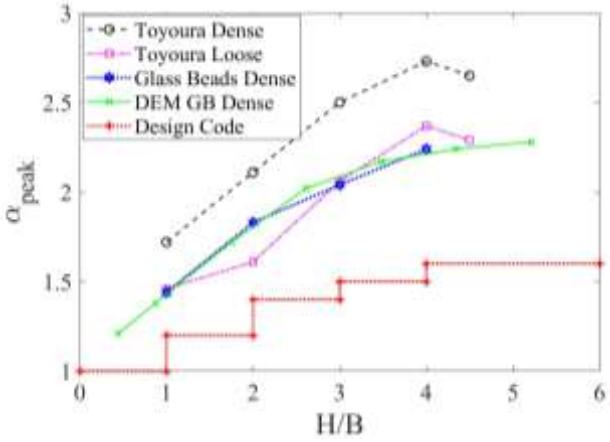

Fig. 8. Comparison of α_{peak} for various cases.

5 CONCLUSIONS

Trapdoor model tests were conducted to understand the earth pressure distribution and the particle scale mechanism of arching using spherical glass beads. Equivalent DEM analyses were performed to validate the experimental observation, and the following conclusions can be drawn:

(1) The vertical earth pressure acting to a buried structure becomes greater than the initial state due to differential settlement between the structure and the surrounding subsoil.

(2) The shear stress acting on a buried structure shows clear peaks at the boundary between the subsoil and the structure when *H/B* is large. In contrast, lower *H/B* causes little change in shear stress distribution.

(3) Uniform settlement of the ground surface was observed for larger *H/B* values at a given width of trapdoor. In contrast, differential settlement was obvious for lower *H/B* values.

(4) The α_{peak} values for experiments using glass beads were lower compared with Toyoura sand at a similar void ratio, whereas a close agreement was observed between the experiments using glass beads and the DEM analyses. Design values of α as considered in the Japan Road Association (1999) are underestimated.

(5) Development of an arch can also be assessed by measuring the α parameter that approaches a critical state value at larger *H/B*; the present trapdoor test approaches α = 2.5 to 3 for the given test scenario.

ACKNOWLEDGEMENTS

Authors are grateful to Prof. Reiko Kuwano, the University of Tokyo for her insight review and constructive suggestions on this paper.

REFERENCES

Chevalier B., Combe G. and Villard P. (2009). Experimental and Numerical Study of the Response of Granular Layer in the Trapdoor Problem. AIP Conference Proceedings 1145, 649.

Costa D. Y., Jorge G. Z., Benedito S. B. and Carina L. C. (2009). Failure Mechanisms in Sand over a Deep Active Trapdoor. Journal of Geotechnical and Geo-Environmental Engineering, 135(11), 1741-1753.

General guidelines for road earthworks – culvert work (1999). Japan road association, ISBN 978-4889504101, Maruzen Print Co. Ltd.

Kuwano, R. and Ebizuka, H. (2010). Trapdoor tests for the evaluation of earth pressure acting on a buried structure in an embankment, Proc. 9th International symposium on new technologies for urban safety of mega cities in Asia, USMCA, Kobe, 453-460.

Plimpton S. (1995). Fast parallel algorithms for short-range molecular-dynamics. Journal of Computational Physics, 117(1), 1–19.

Rui R., Frits V. T., Xiao-Long X., Suzanne V. E., Gang H. and Yuan-you X. (2016). Evolution of soil arching; 2D DEM simulations. Computers and Geotechnics 73, 199-209.